JOURNAL OF SOLID STATE CHEMISTRY **84**, 375–385 (1990)

The Solid Solution $Pb_{0.5}Sr_{2.5}Y_{1-x}Ca_xCu_2O_{7-\delta}$: Superconductivity and Structure

T. ROUILLON, J. PROVOST, M. HERVIEU, D. GROULT, C. MICHEL, AND B. RAVEAU

Laboratoire de Cristallographie et Sciences des Matériaux,
CRISMAT, ISMRa, Université de Caen, Boulevard du Maréchal Juin,
14032 Caen Cedex, France

Received August 2, 1989; in revised form October 23, 1989

The "system" $Pb_{0.5}Sr_{2.5}Y_{1-x}Ca_xCu_2O_{7-\delta}$ has been investigated for its structural and superconducting properties. A pure phase has been isolated for $0 \leq x \leq 0.60$, whose structure belongs to the [2,2] type, i.e., consists of an intergrowth of double pyramidal copper layers ($m = 2$) with double rock salt-type layers containing lead and strontium. The oxides corresponding to $0 \leq x \leq 0.40$ do not superconduct, whereas the pure phases corresponding to $0.50 \leq x \leq 0.60$ exhibit critical temperatures deduced from magnetic measurements ranging from 50 to 75 K, with diamagnetic fraction volumes at 4 K ranging from 8 to 65% in agreement with the $T_C(R = 0) = 53$ K, previously observed for $x = 0.50$ from resistivity measurements. The enhancement of superconductivity by annealing under an oxygen flow is demonstrated. The magnetic study of two phase samples $0.7 \leq x \leq 0.9$ and especially of $x = 0.9$ shows a diamagnetic fraction volume of 3–4%, corresponding to a $T_C = 104$ K, which confirms the possibility of superconductivity up to 100 K in this system. The structural study of these oxides and especially of the nonsuperconducting sample $x = 0$ allows a comparison to be made with the superconductor $x = 0.5$. Although they belong to the same structural type, the first one differs from the second one, by the existence of several superstructures which are interpreted in terms of ordering of lead, strontium, and oxygen vacancies in the rock salt-type layer.

A new superconductor $Pb_{0.5}Sr_{2.5}Y_{0.5}Ca_{0.5}Cu_2O_{7-\delta}$ has been recently isolated (*1*), whose superconducting properties depend upon the thermal treatment, with a $T_C^{on} = 100$ K and $T_C^{off}(R = 0) = 53$ K. The structure of this tetragonal oxide belongs to the "1212" type observed for thallium cuprates (*2*, *3*), i.e., consists of the intergrowth of a double rock salt-type layer $[(AO)_2]_\infty$ with a double oxygen-deficient perovskite layer (Fig. 1). One original feature of this oxide concerns the oxygen deficiency observed in the perovskite layers ($\delta \sim 0.9$–0.5) which may depend upon the thermal treatment and may also influence the superconducting properties of this oxide. The variation of the Y/Ca ratio should also introduce a variation of the oxygen content and possibly of the Cu(II)/Cu(III) ratio so that the superconducting properties of those phases may be affected. We report here on the study of the solid solution $Pb_{0.5}Sr_{2.5}Y_{1-x}Ca_xCu_2O_{7-\delta}$.

Experimental

Samples were prepared from mixtures of PbO_2, PbO, SrO_2, $SrCuO_2$, Y_2O_3, CaO, and CuO in adequate ratios, leading to the nominal composition $Pb_{0.5}Sr_{2.5}Y_{1-x}Ca_x$

0022-4596/90 $3.00

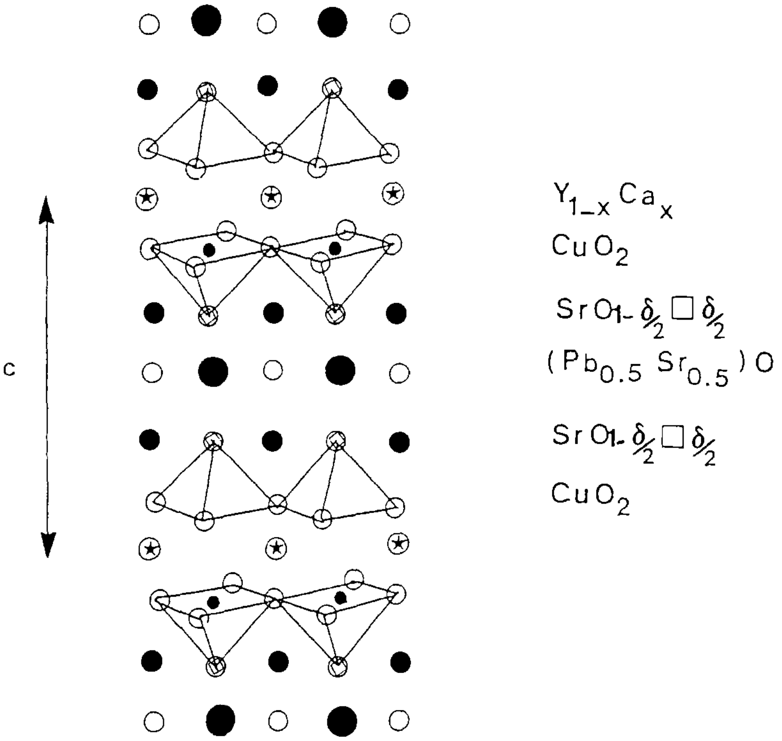

FIG. 1. Schematic drawing of the structure of the superconducting oxide $Pb_{0.5}Sr_{2.5}Y_{1-x}Ca_xCu_2O_{7-\delta}$.

Cu_2O_y. The oxides were intimately crushed, pressed as pellets, and heated in evacuated silica tubes. Different ratios PbO_2/PbO for a constant lead content were used in order to vary the partial pressure of oxygen in the tube; they correspond to different oxygen contents of the nominal compositions. The samples were heated at temperatures ranging from 825 to 950°C, during times ranging from 1 to 10 hr.

Sample homogeneity was checked by X-ray and electron diffraction. X-ray diffraction analysis was performed using an Inel counter and a Philips diffractometer, using Cu$K\alpha$ radiation. The electron diffraction study was performed with a Jeol 120CX electron microscope fitted with a side entry goniometer (±60°). Magnetic measurements were performed using a SQUID magnetometer at temperatures ranging from 5 K to room temperature.

Results and Discussion

Homogeneity Range

With the experimental conditions described above, the best results were obtained for "nominal compositions" corresponding to $7 \leq y \leq 7.25$; however, as it will be shown later, the real oxygen content of the resulting compounds could be smaller than 7.

A solid solution $Pb_{0.5}Sr_{2.5}Y_{1-x}Ca_xCu_2O_{7-\delta}$ is synthesized for $0 \leq x \leq 0.60$. The X-ray powder diffractograms of these oxides were indexed in a tetragonal cell (Table I), in agreement with the electron diffraction study which confirms the space group *P4/mmm*, characteristic of the "1212"-type structure previously established for the superconductive compound $x = 0.50$. It should be noted that the X-ray diffractogram of the limit phase $Pb_{0.5}Sr_{2.5}$

TABLE I

$Pb_{0.5}Sr_{2.5}Y_{1-x}Ca_xCu_2O_{7-\delta}$: PARAMETERS OF THE TETRAGONAL CELL VS x

x	a(Å)	c(Å)
0	3.8253(3)	11.891(1)
0.2	3.8170(6)	11.846(3)
0.4	3.8209(3)	11.887(1)
0.5	3.8166(6)	11.907(3)
0.6	3.8195(7)	11.932(3)

$YCu_2O_{7-\delta}$ ($x = 0$), exhibits very weak extra lines which cannot be indexed in the classical "1212" tetragonal cell and do not belong to any known phase in the diagram such as $Pb_2Sr_2YCu_3O_8$ (*4*); these extra lines can be indexed in the supercells which were observed by electron diffraction ($a_p\sqrt{13} \times a_p\sqrt{13}$). For $x > 0.60$ values, the X-ray diffraction analysis gives evidence of a two-phase mixture: "1212"-type and a phase closely related to Sr_2PbO_4 (*5*) and Ca_2PbO_4 (*6*); the amount of the latter increases with x.

Magnetization Measurements

Magnetic measurements were performed on every sample and checked vs the thermal conditions, i.e., for 825, 875, and 950°C synthesis temperatures and after 400°C annealings under oxygen flow.

Whatever the thermal conditions may be superconductivity was only observed for $0.5 \leq x < 1$.

$x = 0.5$ and $x = 0.6$

Electrical resistance (dc) was measured by a standard four probes technique between 4.2 K and room temperature. Magnetization measurements were performed with a SQUID magnetometer. We report here on two types of magnetic measurements: magnetic moment (zero field cooled) versus temperature under a 10-Oe applied field; and low field ($H \leq 2000$ Oe) magnetization $M(H)$ at $T = 5$ K. Figure 2 shows the ratio $R(T)/R(300\text{ K})$ vs T for $x = 0.5$ and for different synthesis conditions. In this case it can be seen that the best results are obtained for the lower temperature. The magnetic measurements performed on $x = 0.5$ samples before and after annealing under oxygen flow at 400°C during 15 hr are plotted in Figs. 3a and 3b. These curves confirm the resistivity curves and clearly show that the superconducting properties are enhanced by annealing under oxygen flow. The best diamagnetic volume at 5 K is obtained for the sample synthesized at 870°C and then annealed under oxygen flow. But above 15 K the diamagnetic volume is higher for the sample synthesized at 825°C annealed under oxygen. T_C is 60 K for the first and 75 K for the second. The highest superconducting fraction at 5 K under $H = 10$ Oe is due to the peak observed at low field (see inset in Fig. 3b) as outlined in a previous paper (*1*). Figure 3b clearly shows that the 825°C synthesis temperature gives better results than 870°C and that in both cases superconductivity is enhanced by annealing under oxygen flow at 400°C.

These effects are also envidenced for $x = 0.6$ sample. Figures 4a and 4b show for this sample the magnitude of cumulated effects of both synthesis temperature and oxygen annealing. Few tentatives, not reported here, were made for synthesis temperature lower than 825°C and longer synthesis time than 7 hr at 825°C but both damaged superconducting properties.

$x = 0.7$, 0.8, and 0.9

As stated above for these x values samples were not single phased. Resistivity measurements were only possible on $x = 0.7$ and $x = 0.8$ samples. For $x = 0.9$ we observed a diamagnetic signal corresponding to about 4% of the sample volume at 5 K but this sample was found insulating at low temperature. This result is consistent with the increasing volume of the foreign phase leading to an impossibility of percolation

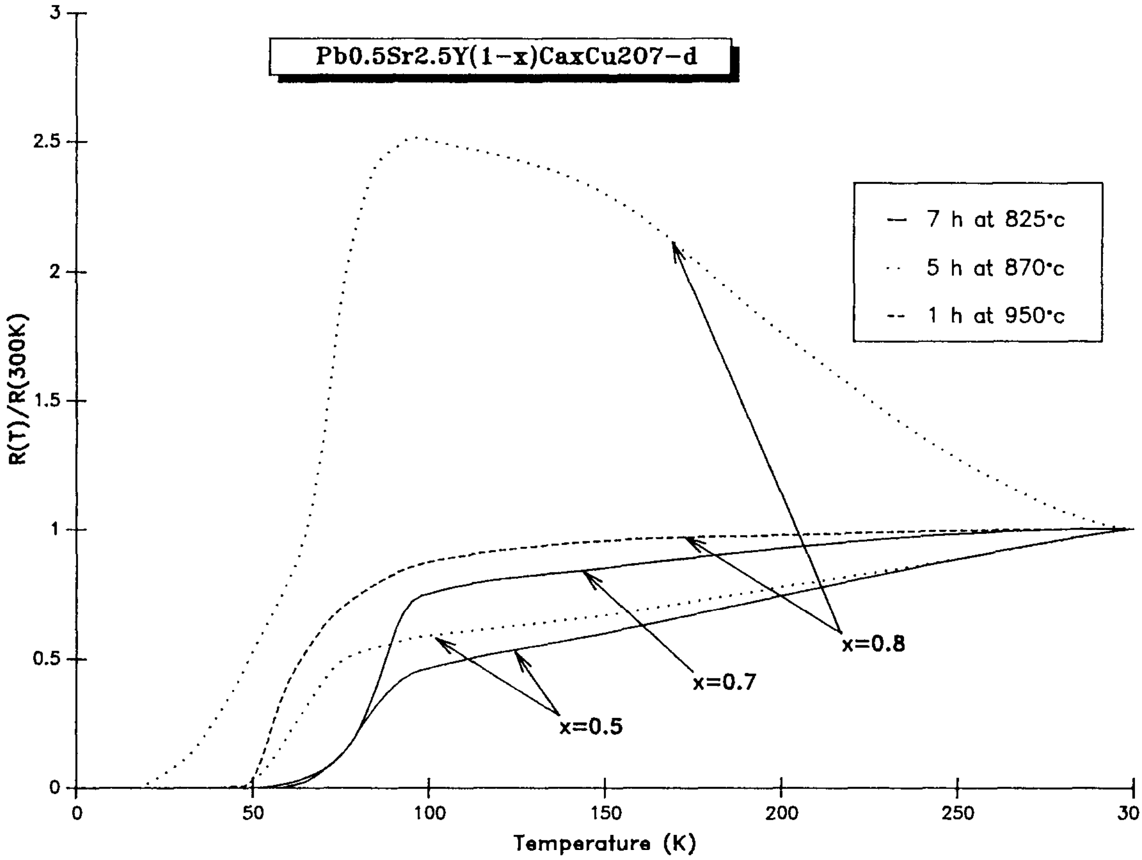

FIG. 2. Temperature dependence of the ratio $R(T)/R(300\text{ K})$ for different x values and for different synthesis conditions (unannealed samples).

between superconducting parts of this sample. $R(T)/R(300\text{ K})$ ratio for $x = 0.7$ and 0.8 are plotted in Fig. 2. Magnetization versus temperature ($H = 10$ Oe) and versus field ($H \leq 2000$ Oe) at 5 K are plotted in Figs. 5a and 5b for $x = 0.7$, in Figs. 6a and 6b for $x = 0.8$, and in Figs. 7a and 7b for $x = 0.9$. These figures show the main following results:

(i) As for the lower x values we found that the superconducting properties are better for the 825°C synthesis temperature.

(ii) These measurements confirm also the enhancement of superconductivity by annealing under oxygen flow.

(iii) An interesting feature is found in Fig. 7a concerning the $x = 0.9$ sample. This sample which is insulator by resistivity measurement presents a diamagnetic signal corresponding to 3–4% of the sample volume and $T_C \sim 104$ K. This result confirms the possibility of superconductivity up to 100 K in this system. This possibility suggested by resistive measurements in our previous preliminary result (*1*) is confirmed by magnetic measurements.

Structural Study

The structural study was performed by both electron and X-ray diffraction techniques.

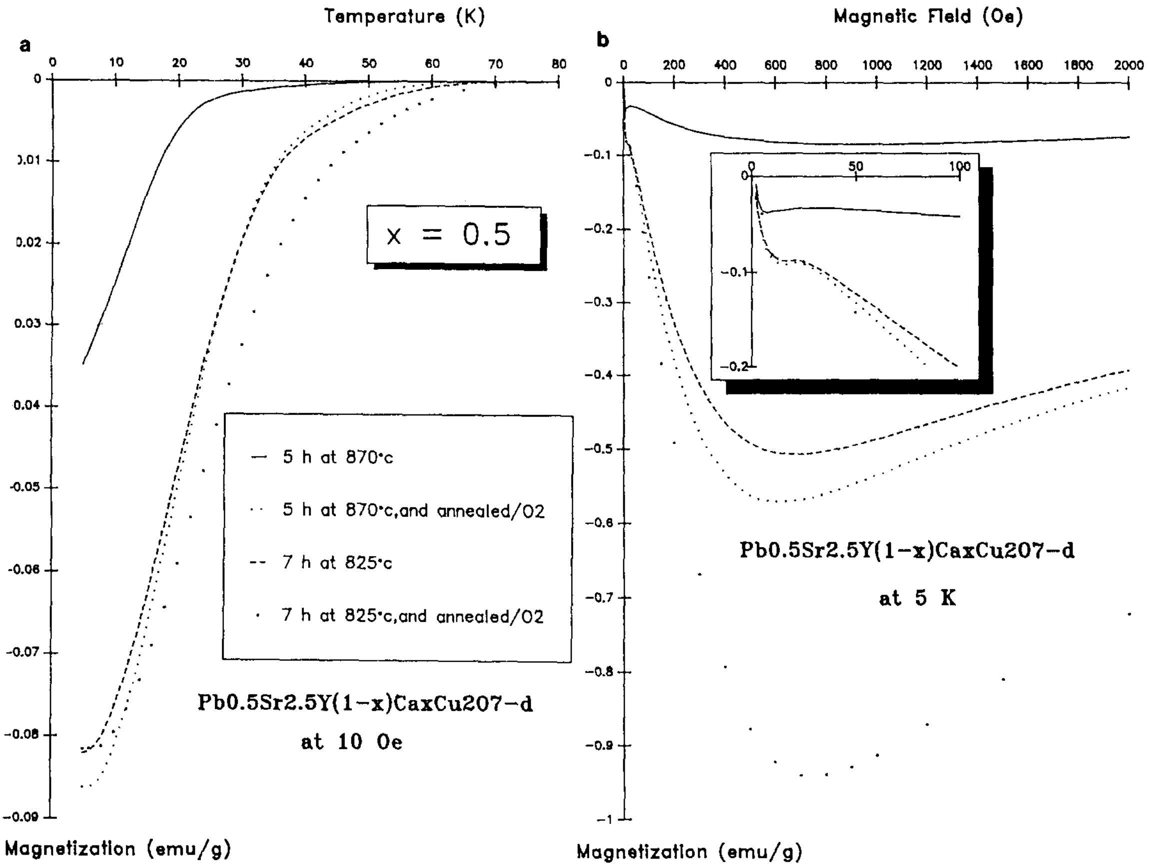

FIG. 3. (a) Magnetization vs T for $Pb_{0.5}Sr_{2.5}Y_{1-x}Ca_xO_{7-\delta}$ ($x = 0.5$) at 10 Oe for different thermal treatments; (b) magnetization vs H ($H < 2000$ Oe) at 5 K for the same samples. Insert shows the low field part of the curves.

A detailed electron diffraction (ED) investigation was performed on three samples corresponding to different compositions and thermal treatments.

—The as-synthesized superconducting sample $Pb_{0.5}Sr_{2.5}Y_{0.5}Ca_{0.5}Cu_2O_{7-\delta}$ ($x = 0.5$, 825°C, 7 hr) exhibits ED patterns similar to those previously described (*1*): the basic reflections are those characteristic of the *P*4/*mmm* space group and numerous satellites are observed lying mainly along ⟨102⟩*, and sometimes along ⟨203⟩*. These extra spots are in almost commensurate positions and their intensities vary from one crystal to the other. Some rare crystals exhibit a double cell ($a\sqrt{2} \times a\sqrt{2}$).

—The same sample, annealed under oxygen flow (15 hr, 400°C), was observed. It appears that the intensity of the extra spots is drastically decreased and that numerous crystals can be considered as free of this feature.

—In the $x = 0$ nonsuperconductive phase, we observe for many crystals additional and intense reflections in commensurate positions. These extra spots set up along various directions leading to different superstructures. Some examples are shown

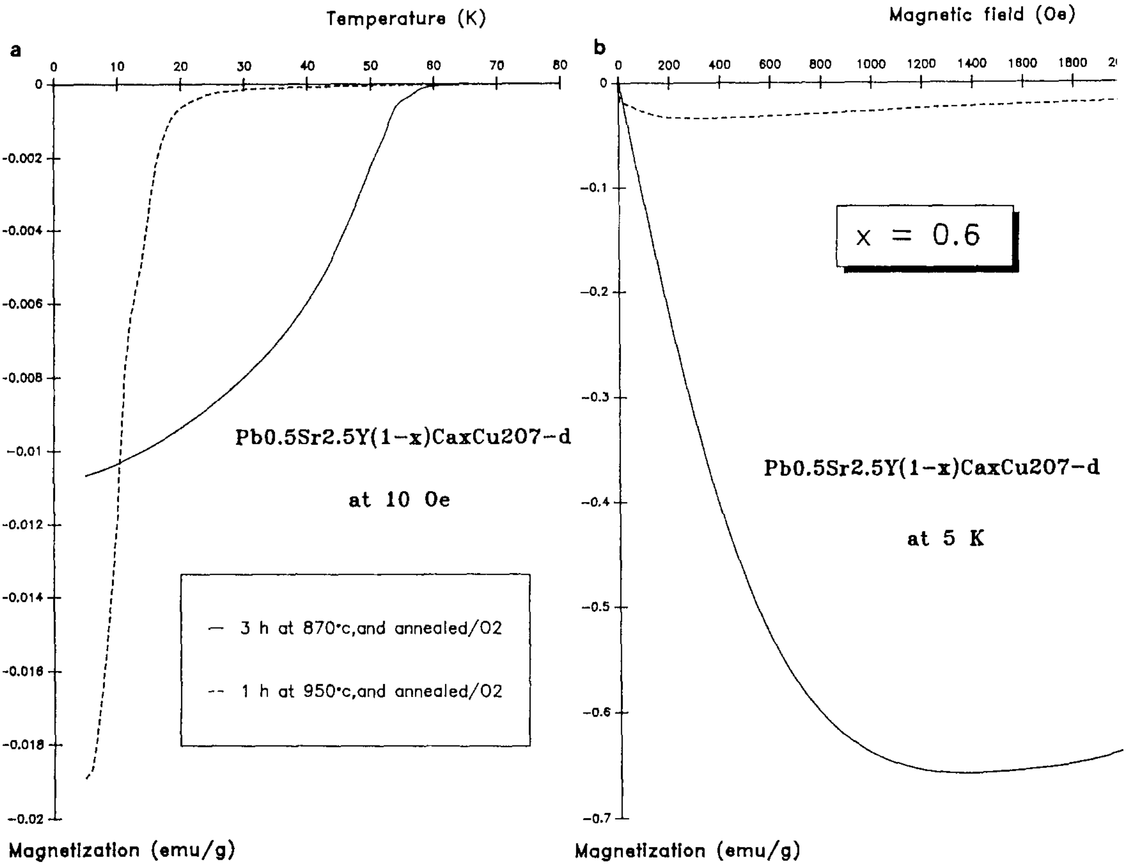

FIG. 4. (a) and (b) Same curves as in legend to Fig. 3 for $x = 0.6$.

in Fig. 8. Weak extra spots are observed along [210]* and [120]* (Fig. 8a), leading to "5 × d_{210}" periodicity, i.e., to a "$a\sqrt{5}$" superstructure. In a great number of patterns strong extra spots appear along [110]* and [1$\bar{1}$0]* (Fig. 8b). More complex patterns are sometimes obtained with extra spots along [230]* leading to 13 × d_{230} superstructures (Fig. 8c) or along [710]* (Fig. 8b). Besides these superstructure reflections, there appear in many [010] patterns satellites along [102]* with $q = 4$ similar to those previously observed for $Pb_{0.5}Sr_{2.5}Y_{0.5}Ca_{0.5}Cu_2O_{7-\delta}$ (*1*) (Fig. 8d); but contrary to this latter phase, the satellites are much weaker, sometimes not observed and those of second order are generally missing.

The determination of the structure of the limit phase $Pb_{0.5}Sr_{2.5}YCu_2O_{7-\delta}$ was performed from the 36 first reflections; i.e., 59 *hkl* of the X-ray diffractogram. Refinements of the positional parameters and occupancy factors of cations were carried out with a thermal factor of oxygen atoms fixed to 1 Å^2. An eventual preferred orientation was taken into account for these calculations but the weak value of the corresponding parameters cannot be considered as significant showing that this phenomenon can be excluded. The discrepancy factor calculated on the intensities was lowered to R =

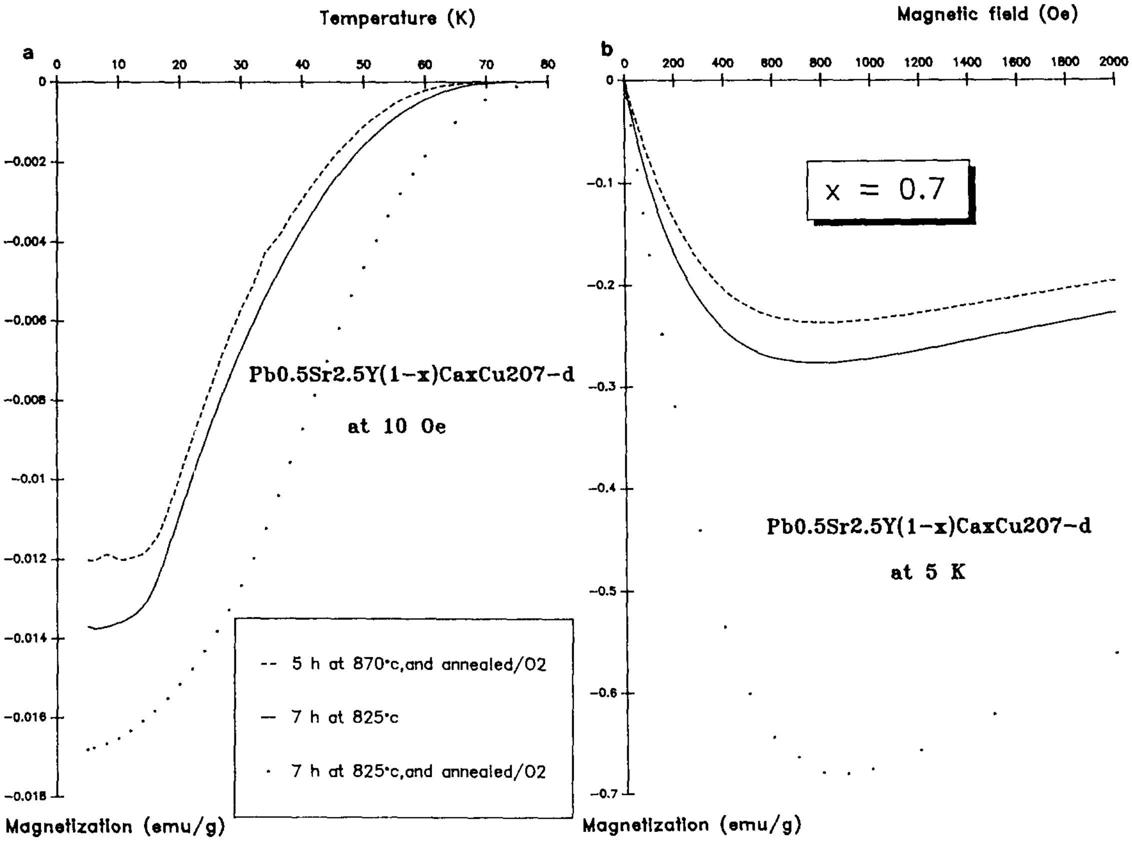

FIG. 5. (a) and (b) Same curves as in legend to Fig. 3 for $x = 0.7$.

0.085 for the atomic coordinates given in Table II. Owing to the possibility of anionic deficiency, the oxygen parameters were then separately refined in order to check the event of an unusual feature. From these calculations, values close to 1.0 were obtained for τ and B factors of the O(1) and O(3) atoms and were then arbitrarily fixed to 1.0 for further refinements. On the contrary, the R value was significantly decreased (from 0.085 to 0.066) by either increasing the B factor (10 Å^2) or decreasing the τ value (0.8) of O(2). The splitting of the x, y positions of the corresponding site (2(h) to 8(r)) was also considered but the resulting values ($x = y = 0.598$) led to unlikely interatomic distances. Although the low scattering factor of oxygen does not allow accurate values to be refined, these results can be considered as significant and attest strong disturbances in the $[SrO]_\infty$ layers correlated with oxygen displacements and/

TABLE II

$Pb_{0.5}Sr_{2.5}YCu_2O_{7-\delta}$: POSITIONAL PARAMETERS

		x	y	z	τ	B (Å)^2
$Pb_{0.5}Sr_{0.5}$	(1d)	0.5	0.5	0.5	1.00(3)	1.9
Sr	(2g)	0.0	0.0	0.2891(8)	1.00(3)	1.0
Y	(1a)	0.0	0.0	0.0	1.00(3)	1.0
Cu	(2f)	0.5	0.5	0.1391(9)	1.00(3)	1.0
O(1)	(4i)	0.0	0.5	0.1235(9)	1.0	1.0
O(2)	(2h)	0.5	0.5	0.308(6)	[a]	[a]
O(3)	(1b)	0.0	0.0	0.5	1.0	1.0

[a] For τ and B values of O(2) see text.

TABLE III

$Pb_{0.5}Sr_{2.5}YCu_2O_{7-\delta}$: INTERATOMIC DISTANCES IN Å

(Pb,Sr)–O	2.71 × 4	Y	2.41 × 8
	2.28 × 2		
		Cu	1.92 × 4
			2.01 × 1
Sr–O	2.75 × 4		
	2.51 × 1		
	2.71 × 4		

or oxygen deficiency. However, they confirm that the structure of the $Pb_{0.5}Sr_{2.5}Y_{1-x}Ca_xCu_2O_{7-\delta}$ phases consists of double layers of corner-sharing CuO_5 pyramids interleaved with yttrium and calcium cations, intergrown with double rock salt-type layers (Table III). The rock salt-type slabs exhibit a particular feature with respect to the classical "1212" type structure: they are built up from a mixed layer $[Pb_{0.5}Sr_{0.5}O]_\infty$ sandwiched by two $[SrO_{1-\delta/2}]_\infty$ layers (Fig. 1).

Moreover, despite the low accuracy of the oxygen refinements it appears that, in these phases, ($0 < x \leq 0.6$) the strontium–oxygen layers which ensure the junction between the rock salt and perovskite-type layers are undoubtly oxygen deficient, even if one takes into account a partial oxidation of Pb^{II} into Pb^{IV}; this oxygen deficiency induces for copper a square planar coordination (Fig. 9a). This resistivity measurements of the oxygen-annealed samples (1.6×10^{-2} and 5 Ω cm for $x = 0.5$ and $x =$

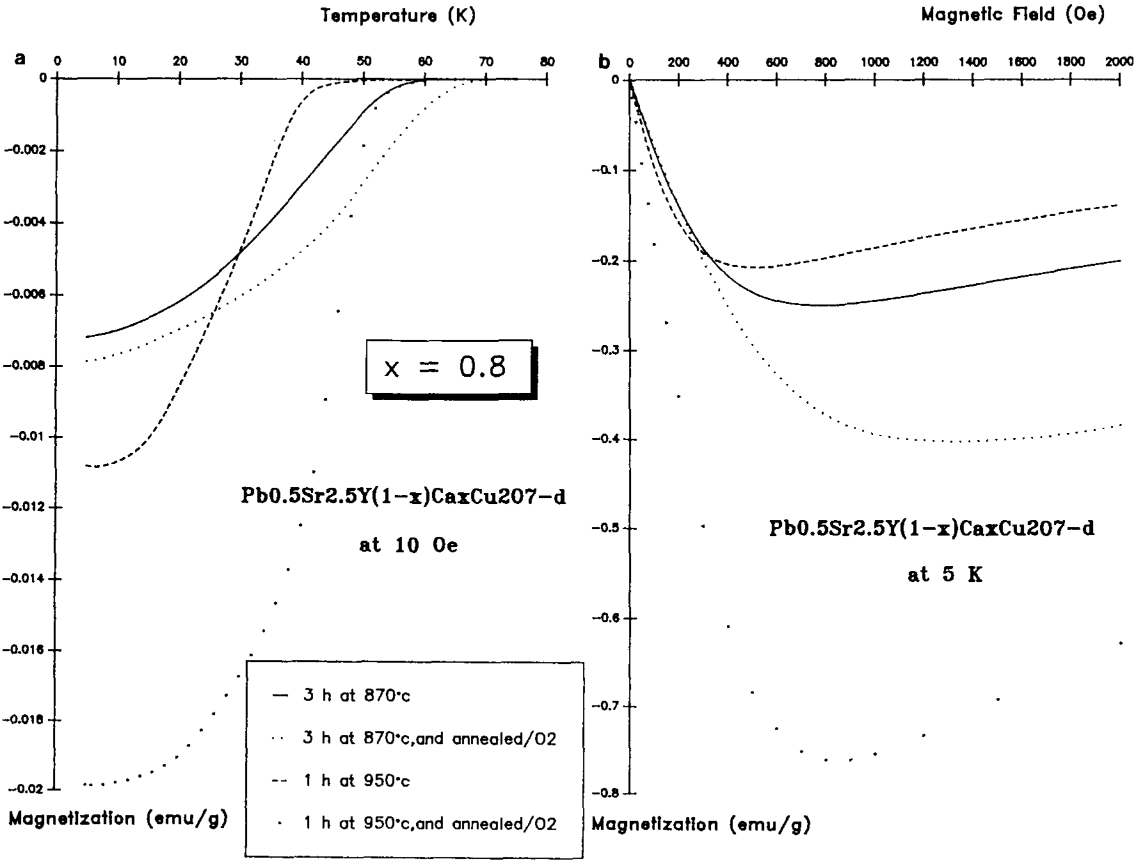

FIG. 6. (a) and (b) Same curves as in legend to Fig. 3 for $x = 0.8$.

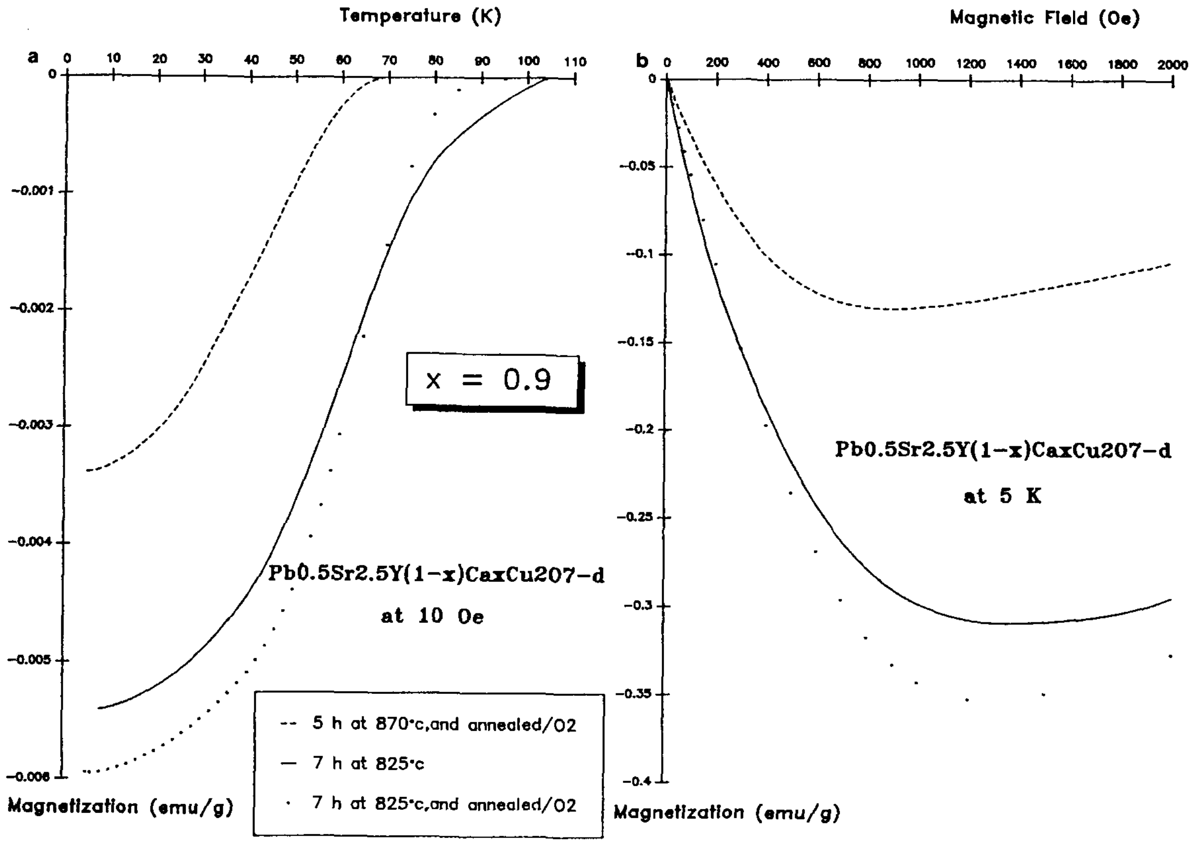

FIG. 7. (a) and (b) Same curves as in legend to Fig. 3 for $x = 0.9$.

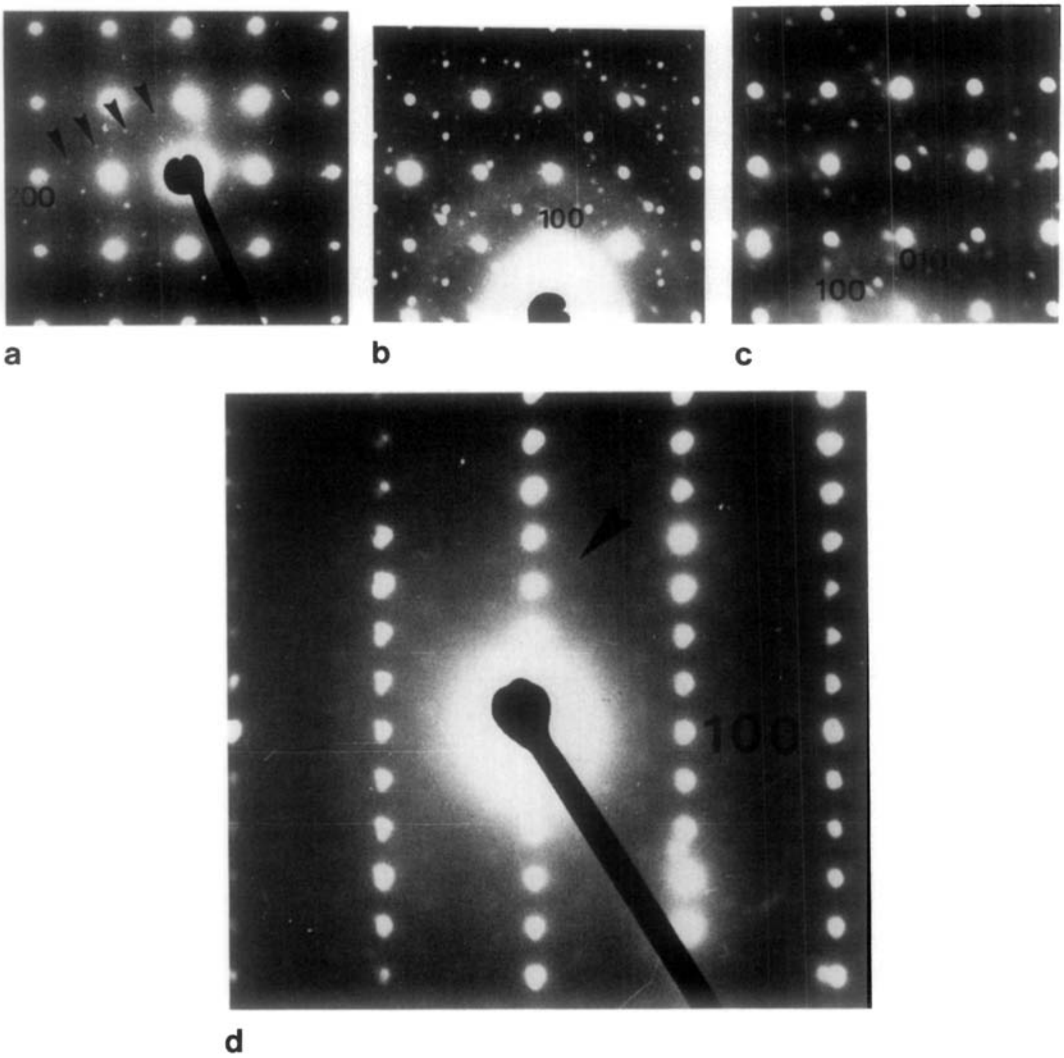

FIG. 8. [001] ED patterns showing extra spots setting up along (a) [210]* direction, (b) [110]*, [1$\bar{1}$0]*, and [710]* directions, and (c) [230]* direction; (d) satellites along [102]* (arrow) with $q = 4$ in a [110] ED pattern.

0, respectively) give evidence of a partial oxidation of copper for both oxides; however, the semiconducting behavior of the $x = 0$ oxide with regard to the metallic behavior of the $x = 0.5$ superconducting oxide attests of a rather small amount of Cu(III) in the yttrium phase $Pb_{0.5}Sr_{2.5}YCu_3O_{7-\delta}$.

The difference in the nature of the extra spots observed in the electron diffraction patterns, mainly satellites in $x = 0.5$ and superstructure spots in $x = 0$, could be generated by different structural features. The satellites which appear in oxygen-deficient oxides could be correlated to the distortion of the rock salt layers and the existence of oxygen vacancies; the superstructures, which are especially observed in the oxygen-rich phases ($x = 0$), could be correlated to orderings of the lead and strontium cations. In that way, the decrease observed in the intensity of the satellites after annealings under oxygen at low temperature and a slow temperature lowering could be explained by a lowering of the distortion of the AO layers correlated with a decrease of the oxygen deficiency and the stereoactivity of the Pb(II) $6s^2$ lone pair (*7*); the extension of the lone pair towards the vacancy positions (Fig. 9b) allows indeed the distortion of the rock salt-type layers to be reduced, by tending again to a pyramidal coordination, CuO_4L (L = lone pair), for copper.

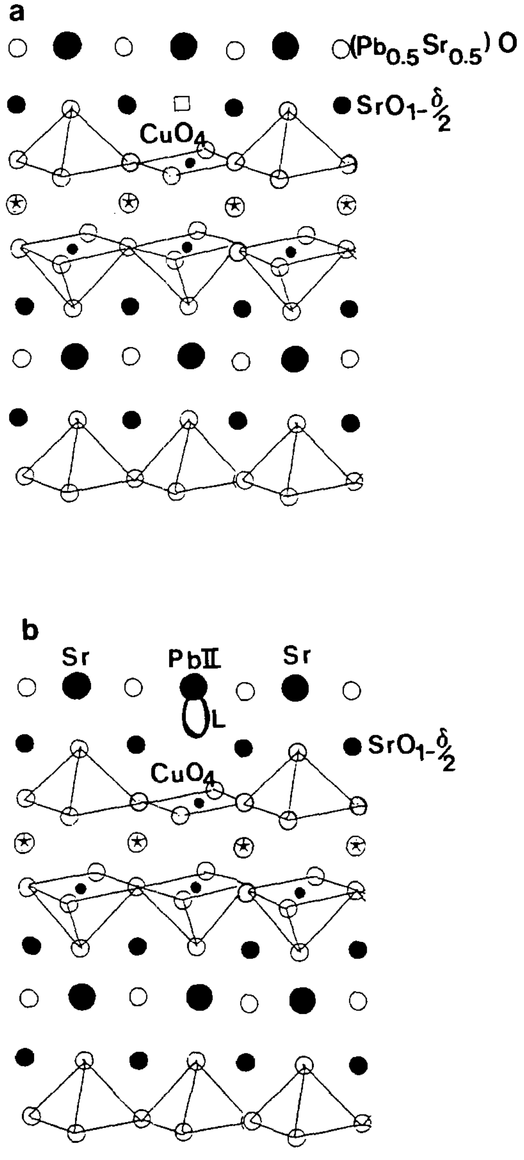

FIG. 9. Schematic drawing of the structure showing the oxygen deficiency of one of the SrO layers leading to copper in a square planar coordination (a). Extension of the $6s^2$ lone pair of Pb(II) towards the oxygen vacancy leading for copper to a pyramidal coordination CuO_4L (b).

Acknowledgment

This work was supported by DRET under Contract 87-1418.

References

1. T. ROUILLON, J. PROVOST, M. HERVIEU, D. GROULT, C. MICHEL, AND B. RAVEAU, *Physica C* **159,** 201 (1989).
2. M. HERVIEU, A. MAIGNAN, C. MARTIN, C. MICHEL, J. PROVOST, AND B. RAVEAU, *J. Solid State Chem.* **75,** 212 (1988).
3. B. MOROSIN, D. S. GINLEY, P. F. HLAVA, M. J. CARR, R. J. BAUGHMAN, J. E. SCHIRBER, E. L. VENTURINI, AND J. K. KWAK, *Physica C* **152,** 413 (1988).
4. R. J. CAVA, B. BATLOGG, J. J. KRAJEWSKI, L. W. RUPP, L. F. SCHNEEMEYER, T. SIEGRIST, R. B. VAN DOVER, P. MARSH, W. F. PECK, JR., P. K. GALLAGHER, S. H. GLARUM, J. H. MARSHALL, R. C. FARROW, J. V. WASZCZAK, R. HULL, AND P. TREVOR, *Nature* (*London*) **336,** 211 (1988).
5. K. L. KEESTER, AND W. B. WHITE, *J. Solid State Chem.* **2,** 68 (1970).
6. M. TROMEL, *Z. Anorg. Allg. Chem.* **371,** 237 (1969).
7. C. MICHEL, C. MARTIN, M. HERVIEU, D. GROULT, D. BOURGAULT, J. PROVOST, AND B. RAVEAU, "Intern. Symp. on Superconductivity, Hsinchu, Taiwan, April 1989," Vol. V, Blue Booklet, Caen, France (1989).